Available online at www.sciencedirect.com
ScienceDirect
Ceramics International 35 (2009) 2443–2447
CERAMICS INTERNATIONAL
www.elsevier.com/locate/ceramint

Impedance spectroscopy analysis of $BaFe_{12}O_{19}$ M-type hexaferrite obtained by ceramic method

Rafael Mendonça Almeida [a], Waldeci Paraguassu [a], Danúbia Soares Pires [b], Ronaldo Ribeiro Corrêa [b], Carlos William de Araujo Paschoal [a,*]

[a] Departamento de Física, Universidade Federal do Maranhão, Campus do Bacanga, 65085-580, São Luis, MA, Brazil
[b] Departamento de Engenharia Elétrica – Centro Federal de Educação Tecnológica do Maranhão, 65030-000, São Luis, MA, Brazil

Received 18 November 2008; received in revised form 20 December 2008; accepted 6 February 2009
Available online 11 March 2009

Abstract

The impedance spectroscopy analysis for M-type $BaFe_{12}O_{19}$ (BaM) ceramics prepared by ceramic route is reported. The main aim is to investigate the electric properties in function of the synthesis parameters (milling time and milling power). It was shown that milling parameters strongly influence the electrical properties such as dielectric constant, whose magnitude increases with the milling power. Moreover the relaxation frequency is fully dependent on the milling parameters and it shifts to high frequencies when milling power decreases. Finally, impedance and dielectric loss tangent also change with milling parameters.

Keywords: A. Milling; C. Dielectric properties; C. Impedance

1. Introduction

Ferrites and garnets are ferromagnetic oxides whose dielectric and magnetic properties allow their use in radio-frequency and microwave applications. Particularly, the high electrical resistivity of ferrites together with their low magnetic losses, minimize the insertion loss in microwave devices and allow their application in magnetic devices. Hexagonal barium hexaferrite ($BaFe_{12}O_{19}$), often denoted as M-type BaM, is widely used in electronics, e.g. permanent magnets, particulate media for magnetic recording [1–4] and microwave devices. These last ones can be found in multilayer chip inductors as the main surface mount devices (SMDs) usually operated in the 0.3–1 GHz frequency range [5].

$BaFe_{12}O_{19}$ hexaferrite crystallizes in a magnetoplumbite structure with space group $P6_3/mmc$. This structure, first observed by Adelsköld [6], consists of a close-packed stacking of oxygen or barium-oxygen layers, with the iron atoms distributed within three kinds of octahedral sites, one tetrahedral site, and one bipyramidal site. The structure is often described in terms of two structural blocks: the spinel S block $(Fe_{11}O_{16})^+$ separated by $(BaFeO_3)^-$ layers, named R block. The Raman spectra for this structure were obtained by Kreisel et al. for BaM single crystals [7] and thin films [8]. For single crystals a detailed group analysis was made. However, at the best of our knowledge, ceramics samples had not been investigated through Raman technique.

The BaM dielectric properties and its solid solutions were extensively investigated, mainly in the microwave range [9–17]. Iwauchi and Ikeda [17] studying hexagonal ferrites showed that M-type ones present low dielectric constant and conductivity in contrast with $BaTi_2Fe_4O_{11}$. The dielectric properties of Sb_2O_3-doped BaM ($BaO_{6-x}Fe_2O_3{\cdot}(Sb_2O)_x$; $x = 0.025$, 0.1 and 0.3) ceramics prepared by conventional ceramic route were investigated by Brahma et al. [9]. These authors showed that the real and imaginary parts of the dielectric constant are drastically changed by the Sb_2O_3 inclusion, even at low concentrations. Two loss peaks were observed and assigned to electric dipole pairs constituted by Fe and Sb. The dielectric constant and conductivity of poly-crystalline samples of $BaCo_{2-x}Zn_xFe_{16-2x}O_{27}$ were studied by Abou El Ata et al. [11,16] for $x \geq 0.4$ at the radiofrequency

* Corresponding author. Tel.: +55 98 2109 8291; fax: +55 98 2109 8204.
E-mail address: paschoal@ufma.br (C.W. de Araujo Paschoal).

0272-8842/$34.00
doi:10.1016/j.ceramint.2009.02.020

range for frequencies higher than 3 kHz. They observed that the a.c. electrical conductivity increases, while the real dielectric constant and dielectric loss decrease, as the angular frequency increases. Besides, they showed that the a.c. conductivity, real dielectric constant and dielectric loss have a minimum when $x \sim 1.2$ due to the Co and Zn ion substitution of Fe ions in the A site that migrates to B site. Ismael et al. [12] investigated the dielectric response of ceramics samples of $BaCo_{2-x}Zn_xFe_{16}O_{27}$ at the radiofrequency range. They showed that the dielectric constant and dielectric loss exhibit dielectric dispersion which agrees well with the Maxwell-Wagner double-layer model. They showed also that these electrical properties increase when the temperature increases. Moreover, they observed a dielectric relaxation in dielectric loss tangent due to the jumping of the charge carriers. The relaxation frequency shifts towards high values when the temperature increases and finally, the dielectric constant, dielectric loss and activation energy for the dielectric relaxation become minimum to 40% of Zinc.

Despite all dielectric and vibrational investigations performed in M-type ceramics, to the best of our knowledge, no analysis of the dielectric properties as function of synthesis conditions in a sample prepared by ceramic route was done. The aim of this work is to investigate the effects of the milling power and milling time in the electric properties of the M-type $BaFe_{12}O_{19}$ ceramics obtained by the ceramic route.

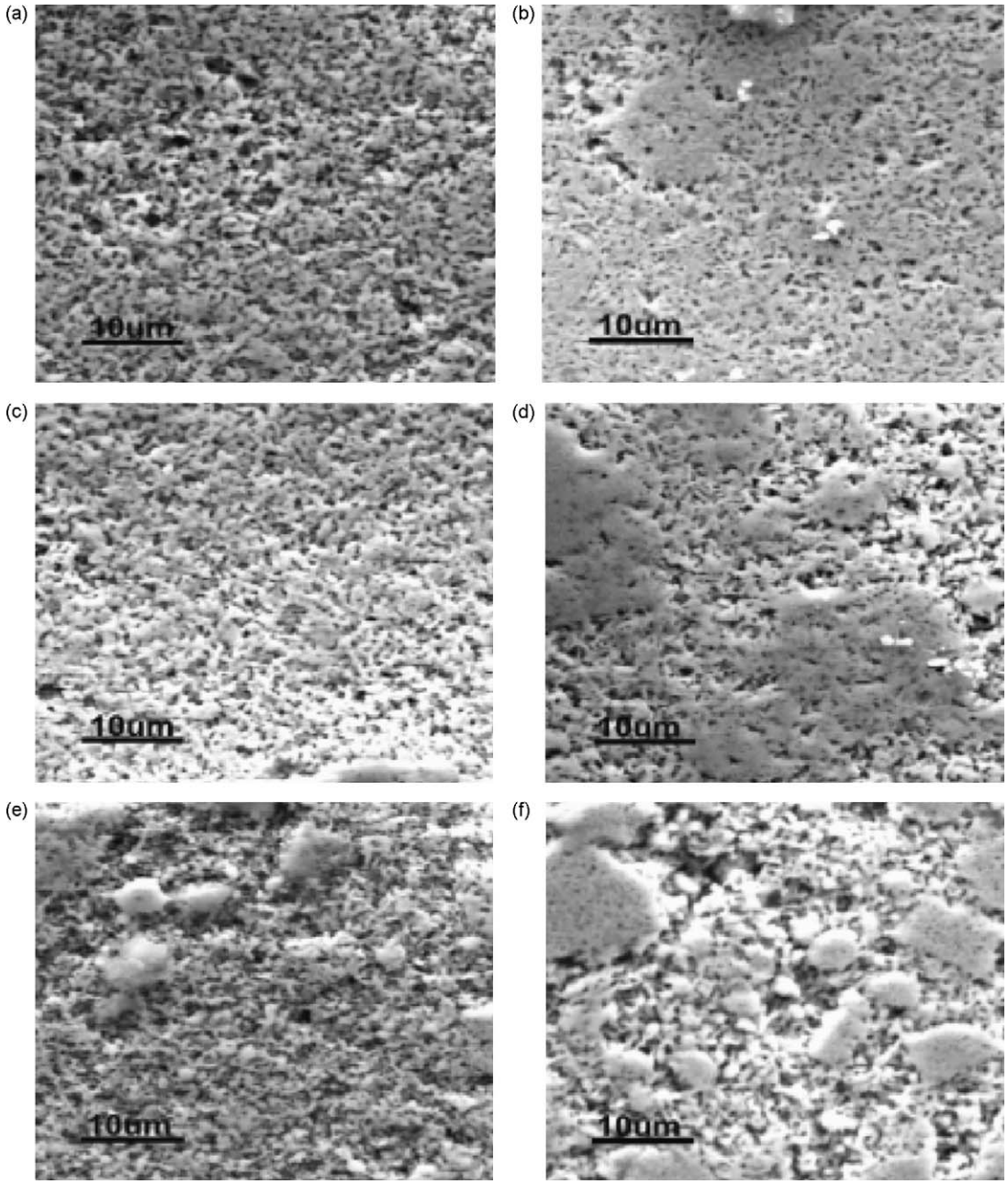

Fig. 1. SEM micrographs of the BaM investigated samples for (a) Pm = 4:1; Tm = 1 h, (b) Pm = 10:1; Tm = 1 h, (c) Pm = 4:1; Tm = 5 h, (d) Pm = 10:1; Tm = 5 h, (e) Pm = 4:1; Tm = 10 h and (f) Pm = 10:1; Tm = 10 h.

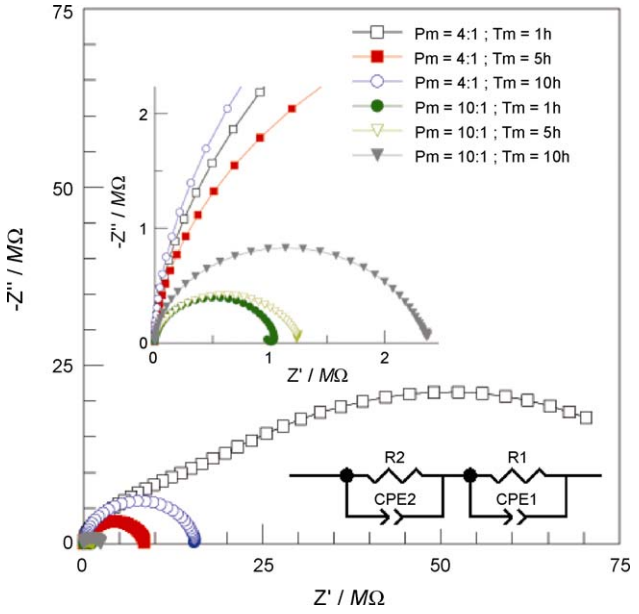

Fig. 2. Nyquist plane for the impedance of the BaM investigated samples. In the insets, we show a zoom for the low impedances and the circuit used to simulate the electrical behavior of the samples.

2. Synthesis and experimental apparatus

The BaM ceramics were prepared by the conventional solid state ceramic route, in which the starting materials were the high-purity $BaCO_3$ (Aldrich Chemicals; 99.9%) and Fe_2O_3 (J.T. Baker Nuclear Fuel Complex, Hyderabad; 99.9). The materials were mixed and ball milled during 10 min. The mixtures were calcined in zirconia crucibles at 1000 °C for 1 h. The calcined powders were mixed thoroughly with 2 wt% PVA solution, and were dried and uniaxially pressed at 2.5 ton with a Schwing Siwa equipment in cylindrical compacts of 17–23 mm in diameter. The pellets were initially heated at a rate of 10 °C/min up to the sintering temperature, where they were kept for 1 h in air. In order to investigate the effects of the intermediary ball milling process, the samples have been milled for three different milling times (1 h, 5 h and 10 h) and milled for two different milling powers (4:1 and 10:1). The six samples were sintered at 1100 °C.

The sample apparent densities were examined using Arquimedes method which consists in the immersion of the synthesized samples in a water volume having its weight modified for the push and porosity gifts.

Scanning electron microscopy was used to determine the morphology, particle size and agglomeration stages of powders. Barium ferrite powders micrographs with milling power of 4:1 and 10:1 were obtained by a Zeiss 940A scanning electron microscopy (SEM).

Impedance spectroscopy measurements were carried out using a frequency response analyzer Solartron model 1260 attached to a dielectric interface Solartron model 1294. The experiments were made using a two-electrode configuration in the frequency range from 1 Hz to 1 MHz. The sample surfaces were painted with silver electrodes in order to form a plane capacitor. For all samples, the thicknesses of the samples were small enough to avoid border effects.

3. Results and discussion

The BaM theoretical density is 4.90 g cm^{-3}. The apparent density obtained for the investigated samples is showed in Table 1. We could observe densities between 3.17 g cm^{-3} and 4.58 g cm^{-3}, where the highest value was obtained for the milling power of 10:1 and milling time of 1 h, while the lowest value was obtained for the milling power of 4:1 and milling time of 5 h. The SEM micrographs of the BaM investigated

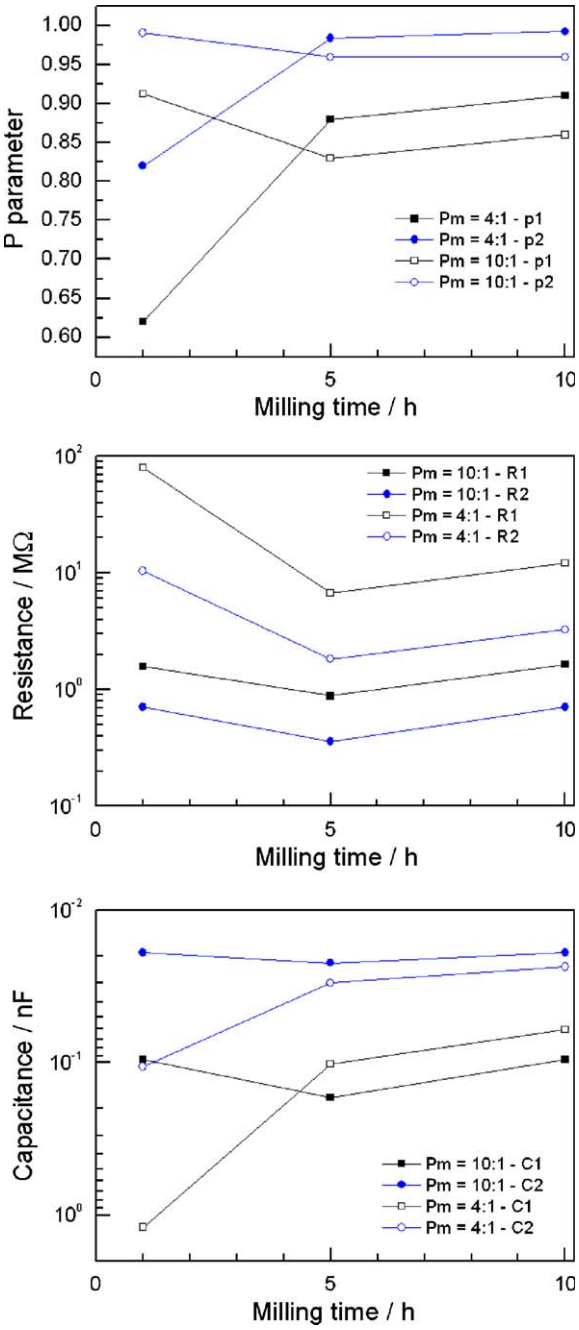

Fig. 3. Milling time dependence of the circuit parameters for the BaM investigated samples.

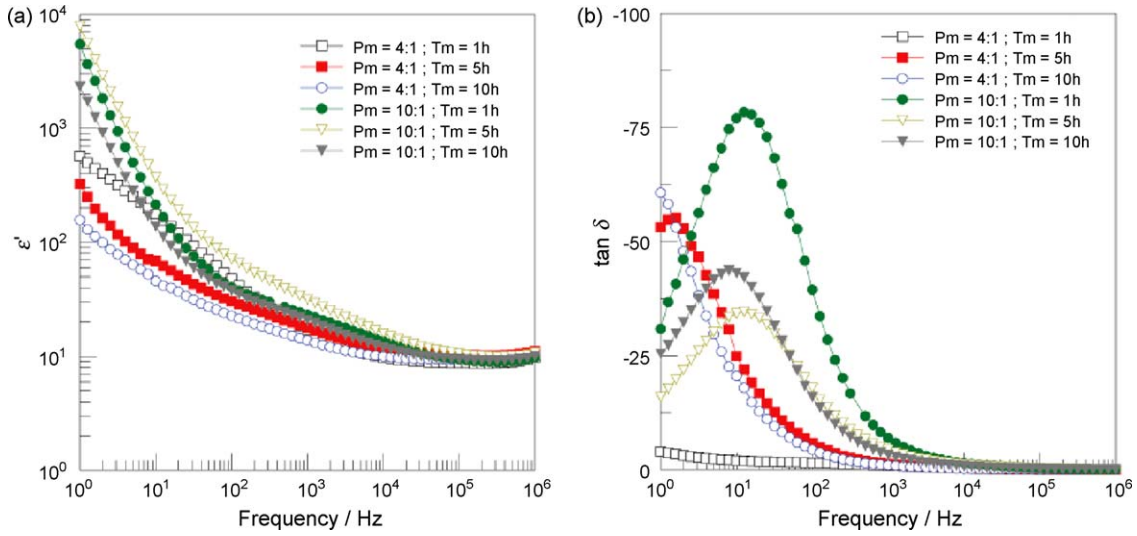

Fig. 4. Dielectric (a) constant and (b) loss of the BaM investigated samples.

samples are showed in Fig. 1. It is observed that at high milling times (Mt = 10 h) there are many agglomerates. Conversely more pores for low milling time and milling power.

Fig. 2 shows the impedance Nyquist plot of the investigated samples. As can been seem, only for the lowest milling time and milling power the impedance arc exhibits two depressed semicircle. This behavior is typical of polycrystalline samples [18]. The electrical model that describes this behavior is a series combination of two circuits each one constituted of a resistor and a constant phase element in parallel [18] (see the circuit in Fig. 2), tone for the bulk and another for the grain boundary contribution. All the samples impedance plots were assigned to this circuit. The CPE element, whose impedance assumes the form

$$Z_{\mathrm{CPE}} = \frac{1}{(j\omega)^{p}C}, \tag{1}$$

models the impedance arcs whose center is not in the Z' axes. Clearly, the higher is the milling power (Mp = 10:1) the lower is the impedance, as can be seen in the inset of Fig. 2.

The milling time dependence with the circuit parameters is showed in Fig. 3. It is observed for 10:1 milled samples that increasing the milling time the p parameter decreases. The agglomerates that arise for low milling times are responsible for the inhomogeneities in grain distribution together with the high density obtained for Mt = 1 h. For Mp = 4:1 the behavior is not the same because for high milling times high p parameters occur. For this milling power, since the density is practically the same for all samples, it is likely that a more homogeneous grain distribution is taking place. The capacitance follows the inverse behavior of the p parameter and the resistance decreases when the time milling increases.

Table 1
Apparent density of the BaM investigated samples.

Sample	Apparent density/g cm^{-3}	Percent/%
Pm = 4:1; Tm = 1 h	3.23	65.9
Pm = 4:1; Tm = 5 h	3.17	64.7
Pm = 4:1; Tm = 10 h	3.32	67.8
Pm = 10:1; Tm = 1 h	4.58	93.5
Pm = 10:1; Tm = 5 h	3.47	70.8
Pm = 10:1; Tm = 10 h	3.19	65.1

Fig. 4 shows the dielectric constant and dielectric loss for all investigated samples. It is observed that the higher is the milling power the higher is the dielectric constant. This behavior is probably related to the close relation between milling power and density [13]. Analyzing the milling time influence for Mp = 10:1, it can be seen that the highest dielectric constant does not occurs for Mt = 10 h. Thus, we can deduce that another effects, different from the bulk polarizations (associated to the high densities), is present. Probably, this effect is due to the boundary effects. It can be seen that the highest value occurs for Mt = 5 h. On the other hand, samples milled for 1 h always shows the lowest dielectric constants for each milling power. The loss shows clearly a relaxation process to samples obtained

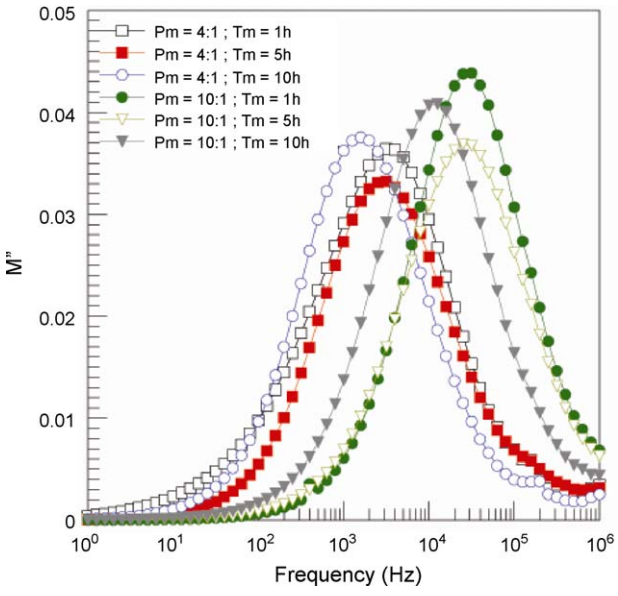

Fig. 5. Imaginary part of the electric modulus of the investigated BaM samples.

with Pm = 10:1. In order to better investigate this relaxation, it is showed in Fig. 5 the imaginary part of the electric modulus once that it is a suitable variable to investigate relaxations in polycrystalline samples [18]. As one can clearly see, there is a relaxation process whose frequency depends of the milling time and power. For any milling power, the relaxation frequency decreases when the milling time increases.

4. Conclusions

The electrical properties of the BaM samples sensibly depend of the synthesis parameters (milling power and milling time). For low milling power, high densities samples do not have the highest dielectric constant. The polarization generated from the boundary grain contributes to a higher dielectric constant for intermediate milling times samples. A relaxation is clearly observed and depends strongly on the milling power. In addition, it could be shown that increasing milling time the resonance frequency decreases.

Acknowledgements

The authors are grateful to the CNPq, FINEP and FAPEMA Brazilian founding agencies.

References

[1] H. Pfeiffer, R.W. Chantrell, P. Gornert, W. Schuppel, E. Sinn, M. Rosler, Properties of barium hexaferrite powders for magnetic recording, Journal of Magnetism and Magnetic Materials 125 (3) (1993) 373–376.
[2] G. Turilli, A. Paoluzi, Magneto and magnetooptical recording materials, Ceramics International 19 (5) (1993) 353–361.
[3] H. Stäblein, in: E.P. Wohlfarth (Ed.), Ferromagnetic Materials: A Handbook on the Properties of Magnetically Ordered Substances, North-Holland, 1982.
[4] S. Capraro, J.P. Chatelon, M. Le Berre, H. Joisten, T. Rouiller, B. Bayard, D. Barbier, J.J. Rousseau, Barium ferrite thick films for microwave applications, Journal of Magnetism and Magnetic Materials 272 (2004) E1805–E1806.
[5] H.M. Sung, C.J. Chen, W.S. Ko, H.C. Lin, Fine powder ferrite for multilayer chip inductors, IEEE Transactions on Magnetics 30 (6) (1994) 4906–4908.
[6] V. Adelsköld, X-ray studies on magnetoplumbite, $PbO{\cdot}6Fe_2O_3$ and other substances resembling 'beta-alumina', $Na_2O{\cdot}11Al_2O_3$, Arkiv før Kemi Mineralogioch Geologi, Series A-12 29 (1938) 1–9.
[7] J. Kreisel, G. Lucazeau, H. Vincent, Raman spectra and vibrational analysis of $BaFe_{12}O_{19}$ hexagonal ferrite, Journal of Solid State Chemistry 137 (1) (1998) 127–137.
[8] J. Kreisel, S. Pignard, H. Vincent, J.P. Senateur, G. Lucazeau, Raman study of $BaFe_{12}O_{19}$ thin films, Applied Physics Letters 73 (9) (1998) 1194–1196.
[9] P. Brahma, S. Banerjee, D. Chakravorty, Dielectric properties of Sb_2O_3-doped $BaFe_{12}O_{19}$ ferrite, Journal of Applied Physics 98 (6) (2005) 064103.
[10] M.C. Dimri, S.C. Kashyap, D.C. Dube, Electrical and magnetic properties of barium hexaferrite nanoparticles prepared by citrate precursor method, Ceramics International 30 (7) (2004) 1623–1626.
[11] A.M.A. Elata, M.A. Elhiti, Dielectric behavior in BaCo2xZnxFe12-2xO19, Journal de Physique Iii 7 (4) (1997) 883–894.
[12] H. Ismael, M.K. Elnimr, A.M.A. Elata, M.A. Elhiti, M.A. Ahmed, A.A. Murakhowskii, Dielectric behavior of hexaferrites Baco2-Xznxfe16O27, Journal of Magnetism and Magnetic Materials 150 (3) (1995) 403–408.
[13] K.K. Mallick, P. Shepherd, R.J. Green, Dielectric properties of M-type barium hexaferrite prepared by co-precipitation, Journal of the European Ceramic Society 27 (4) (2007) 2045–2052.
[14] P. Shepherd, K.K. Mallick, R.J. Green, Dielectric properties of cobalt substituted M-type barium hexaferrite prepared by co-precipitation, Journal of Materials Science-Materials in Electronics 18 (5) (2007) 527–534.
[15] H.J. Zhang, X.L. Jia, X. Ya, L.Y. Zhang, Preparation, dielectric and magnetic properties of barium-ferrite-containing microcrystalline glass ceramic by citrate sol–gel process, High-Performance Ceramics Iii 280–283 (Pts 1 and 2) (2005) 457–460.
[16] A.M.A. El Ata, M.A. El Hiti, M.K. El Nimr, Room temperature electric and dielectric properties of polycrystalline BaCo2xZnxFe12-xO19, Journal of Materials Science Letters 17 (5) (1998) 409–413.
[17] K. Iwauchi, Y. Ikeda, Dielectric-properties of hexagonal ferrites, Physica Status Solidi A-Applied Research 93 (1) (1986) 309–313.
[18] J.R. Macdonald, E. Barsoukov, Impedance Spectroscopy: Theory, Experiment and Applications, Second edition, Wiley–Interscience, 2005.